



The dysfunction of hormone-sensitive lipase induces lipid deposition and reprogramming of nutrient metabolism in fish

Jin-Gang Wang, Si-Han Zhao, Yu-Cheng Qian, Yi-Fan Qian, Yi-Chan Liu, Fang Qiao, Yuan Luo, Mei-Ling Zhang and Zhen-Yu Du*

LANEH, School of Life Sciences, East China Normal University, Shanghai, People's Republic of China

(Submitted 6 July 2022 – Final revision received 22 October 2022 – Accepted 8 November 2022 – First published online 21 November 2022)

Abstract

Hormone-sensitive lipase (HSL) is one of the rate-determining enzymes in the hydrolysis of TAG, playing a crucial role in lipid metabolism. However, the role of HSL-mediated lipolysis in systemic nutrient homeostasis has not been intensively understood. Therefore, we used CRISPR/Cas9 technique and Hsl inhibitor (HSL-IN-1) to establish *hsla*-deficient (*hsla*^{-/-}) and Hsl-inhibited zebrafish models, respectively. As a result, the *hsla*^{-/-} zebrafish showed retarded growth and reduced oxygen consumption rate, accompanied with higher mRNA expression of the genes related to inflammation and apoptosis in liver and muscle. Furthermore, *hsla*^{-/-} and HSL-IN-1-treated zebrafish both exhibited severe fat deposition, whereas their expressions of the genes related to lipolysis and fatty acid oxidation were markedly reduced. The TLC results also showed that the dysfunction of Hsl changed the whole-body lipid profile, including increasing the content of TG and decreasing the proportion of phospholipids. In addition, the systemic metabolic pattern was remodelled in *hsla*^{-/-} and HSL-IN-1-treated zebrafish. The dysfunction of Hsl lowered the glycogen content in liver and muscle and enhanced the utilisation of glucose plus the expressions of glucose transporter and glycolysis genes. Besides, the whole-body protein content had significantly decreased in the *hsla*^{-/-} and HSL-IN-1-treated zebrafish, accompanied with the lower activation of the mTOR pathway and enhanced protein and amino acid catabolism. Taken together, Hsl plays an essential role in energy homeostasis, and its dysfunction would cause the disturbance of lipid catabolism but enhanced breakdown of glycogen and protein for energy compensation.

Key words: Hormone-sensitive lipase: Lipolysis: Energy homeostasis: Glycogen utilisation: Protein metabolism: Zebrafish

Lipid metabolism plays an important role in maintaining energy homeostasis, and its disorder causes some metabolic diseases such as fatty liver, type 2 diabetes and cardiovascular disease^(1–4). Lipolysis, also called hydrolysis of TAG, is the core process of lipid metabolism⁽⁵⁾, and it is defined as the biochemical process by which TAG is broken down into fatty acids (NEFA) and glycerol under the function of multiple enzymes^(6,7). The three main neutral lipases: adipose triglyceride lipase (ATGL), hormone-sensitive lipase (HSL) and monoglyceride lipase participate in the process of hydrolysing TAG into FA⁽⁸⁾. The first step of TAG hydrolysis was catalysed by ATGL to provide FA and diglycerides (DG)^(9,10). HSL also have the capacity of hydrolysing TAG to DG, but it is mainly responsible for the hydrolysis of DG to monoglycerides (MG)^(11–13). Monoglyceride lipase, as its name indicates, hydrolyses MG to FA and glycerol⁽¹⁴⁾. Lipolysis is a critical process controlling the mobilisation and storage of TAG. Unlike ATGL and monoglyceride lipase, HSL is the only lipase directly regulated by neuro-humoral signalling^(15,16). The regulatory domain of HSL has sites of reversible phosphorylation and could be regulated by the cAMP/PKA pathway⁽¹⁵⁾. Pro- and anti-lipolytic hormones, such as catecholamines and

insulin, respectively, can control the intracellular levels of cAMP to regulate the activity of cAMP-dependent protein kinase (PKA). PKA can lead to phosphorylation of HSL to increase its translocation from cytosol to the face of lipid droplets, significantly enhancing its lipolysis activity by conformational changes⁽⁸⁾. In addition, HSL shows a wide range of substrates as it effectively hydrolyses tri-, di- and monoglycerides, even cholesterol, and others substrates^(17,18). All these features give HSL a key role in basal and stimulated lipolysis.

In humans, the clinical characteristics of the carrier with mutated *HSL* gene were firstly reported to be dyslipidemia, hepatic steatosis, systemic insulin resistance and diabetes⁽¹⁹⁾. Similarly, systemic *Hsl*-deficient mice have a higher risk of insulin resistance, hepatic steatosis and inflammation, showing that metabolic dysregulations in *Hsl*-deficient mice are also mainly driven by impaired Hsl function^(20,21). In addition, adipose-specific *Hsl* deficiency mice showed hepatic steatosis, lipodystrophy, macrophage infiltration, and impaired FA oxidative activity⁽²²⁾. Some research has reported that *Hsl*-deficient mice showed greater susceptibility to obesity and lower ability to increase lipolysis under fasted or stimulated conditions^(23,24).

Abbreviations: ATGL, adipose triglyceride lipase; DG, diglyceride; HSL, Hormone-sensitive lipase; MG, monoglycerides.

* **Corresponding author:** Zhen-Yu Du, email zydu@bio.ecnu.edu.cn



Therefore, it is no doubt that HSL is the essential enzyme for the maintenance of energy homeostasis.

The metabolic patterns of different nutrients always keep a relative dynamic balance to maintain energy homeostasis⁽²⁵⁾. Changes in some key enzymes/proteins of lipid metabolism would inevitably lead to a remodelling of overall nutrient metabolism^(26,27). For example, the deficiency of PPAR α , which is a nuclear receptor to regulate lipid catabolism genes⁽⁵⁾, reduced glucose utilisation and expressions of the genes related to glucose transporter, uptake and glycolysis^(26,28). However, inhibiting the synthesis of L-carnitine, which plays a critical role in transporting long-chain fatty acids from the cytosol into mitochondria for fatty acid oxidation⁽²⁹⁾, could promote glucose utilisation and protein deposition through energy homeostasis remodelling in fish⁽³⁰⁾. In the mice, the global deficiency of *Atgl* improved glucose and insulin tolerance and exhibited a better glucose uptake⁽³¹⁾. These studies have shown the functions of different enzymes/proteins in the overall nutrient metabolism. However, as an important lipolysis enzyme, the functions of HSL in overall metabolism have not been evaluated in detail. Therefore, studying the effects of HSL on lipid, carbohydrate and protein metabolism could help people to further understand the nutritional regulatory functions of HSL.

Zebrafish (*Danio rerio*) is a classical animal model being widely used in human disease research and the elucidation of fundamental biological questions^(32–35). Therefore, we choose zebrafish as a model to explore the systemic nutrient metabolism when *hsl* gene was knocked out. This could provide a theoretical basis for understanding the nutritional regulation of Hsl. In addition, excessive fat accumulation is already a severe problem in current aquaculture, causing many adverse effects, including lowered growth, metabolic disorders, impaired immune functions and stress resistance for farmed fish^(36,37). Hence, how to promote the ability of fish to mobilise fat has been a hot area for fish physiologists. Previous studies have shown that Hsl presents in fish and performs a similar lipolytic function to that of mammals^(38–40). In addition, the fish with excessive fat deposition are often accompanied by abnormal *hsl* expression^(41–44). Therefore, using zebrafish as a model to explore the functions of Hsl in fish could also help to understand the regulatory mechanisms of fish lipid metabolism. In the present study, we used either *hsla*-knockout or Hsl enzyme activity inhibitor to construct zebrafish models with Hsl dysfunction. By measuring the growth, swimming activity, oxygen consumption rate, biochemical changes, and the expressions of key genes and proteins in lipid, glucose and protein metabolism, the present study is the first to examine the roles of Hsl in systemic nutrient metabolism.

Materials and methods

Animal ethical approval

All animals were conducted following the Guide for the Care and Use of Laboratory Animals formulated by the Ministry of Science and Technology of China. The study was approved by the Committee on Ethics of Animal Experiments of East China Normal University (Approval ID: F20190101).

Animal source and maintenance

All adult zebrafish (0.4 to 0.5 g) with six months of age were obtained from the Institute of Hydrobiology, Chinese Academy of Sciences (Wuhan, China). Fish were maintained in a recirculating water system with mechanical filtration, and the cycle of 14 h light and 10 h dark at 28°C. After mating between healthy adult zebrafish, fertilised eggs were obtained to be kept in Petri dishes with static water at 28°C. Zebrafish larva were transferred to a recirculating water system 15 d post-fertilisation to feed twice a day with freshly hatched *Artemia salina*.

Establishment of *hsla*-knockout zebrafish line

The *hsla*-knockout zebrafish (*lipea*, NCBI: <https://www.ncbi.nlm.nih.gov/gene/568368>) were established using the CRISPR/Cas9 technique as described in our previous study⁽³³⁾. The CRISPR/Cas9 target sites were designed using the online tool (ZiFiT Targeter version 4.2, <http://zifit.partners.org/ZiFiT/>). The Cas9 messenger RNAs were obtained by *in vitro* transcription from pCS2-nCas9n using the mMESAGE mMACHINE T3 kit (Invitrogen). Double-strand DNA for specific gRNA synthesis was amplified by PCR from pT7-gRNA. The target single-guide RNAs (sgRNAs) was produced using TranscriptAid™ T7 High Yield Transcription Kit (Thermo Scientific). T Cas9 messenger RNA and sgRNA were mixed in proportion and injected into one-cell-stage embryos using the PicoLiter Microinjector PLI-100A (Warner Instruments). The F0 founders carrying mosaic mutations were identified by high-resolution melt analysis and heteroduplex motility assay and mated with WT zebrafish to produce heterozygous F1 offspring. The heterozygotes were allowed to self-cross to acquire the homozygous mutants (F2), resulting in the deletion of –7 bp fragment on the target sites (online Supplementary Fig. 1). The *hsla* mutation locus was confirmed by genomic DNA sequencing. After the natural mating of F2, the homozygous *hsla* knockout (*hsla*^{–/–}) line (F3) was obtained to produce enough offspring for the subsequent experiment.

Experimental design

To explore the role played by Hsl in zebrafish metabolic homeostasis, we used gene knockout and Hsl inhibitor separately to verify the effects of Hsl dysfunction on systemic nutrient metabolism. In the present study, only male zebrafish was used consistently for experiments to avert the effect of sex difference.

For the first experiment, the constructed *hsla*-knockout zebrafish were raised with *Artemia salina* to mature for 3 months. The obtained ninety male zebrafish of each genotype with similar weight (WT and *hsla*^{–/–}: 38 ± 1 mg) were allocated randomly to three 200-litre aquariums for the growth trial (*n* 3). All tanks were conducted in a recirculating system. Both WT and *hsla*^{–/–} fish were fed with a purified basic diet at a feeding rate of 4% body weight two times per d (10.00 and 18.00) for 5 weeks. The formulation of the basic diet is presented in the Table 1. Casein was used as the basic dietary protein source. Soyabean oil was used as the basic dietary lipid source. Dietary ingredients were ground into fine powder. All the ingredients were thoroughly mixed with soyabean oil firstly, and then

Table 1. The formulation and proximate composition of the basic diet and wheat flour dough particles and their composition analysis

Dietary ingredient (%)	Normal diet
Casein	30
Gelatin	5
Corn starch	35
Soyabean oil	7
Vitamin premix*	0.4
Mineral premix†	0.8
Choline chloride	0.5
Butylated hydroxytoluene	0.02
Dimethyl-beta-propiethetin	0.1
Ca(H ₂ PO ₄) ₂	1
Carboxymethyl cellulose	4
Cellulose	16.18
Total	100
Nutrients compositions:	
Moisture (%)	8.61
Total protein (%)	32.84
Total fat (%)	7.66
Total starch (%)	34.33
Ash (%)	2.89
Wheat flour component (%)	
Total protein	12.2
Total fat	1.5
Carbohydrate	70

* Vitamin premix (mg/kg): 500 000 mg retinyl acetate; 50 000 mg cholecalciferol; 2500 mg all-rac- α -tocopheryl acetate; 1000 mg menadione nicotinamide bisulfite; 5000 mg thiamine hydrochloride; 5000 mg riboflavin; 5000 mg pyridoxine; 5000 μ g cobalamin; 25 000 mg inositol; 10 000 mg pantothenic acid, 100 000 mg choline; 25 000 mg niacin; 1000 mg folic acid; 250 mg biotin; 10 000 mg ascorbic acid.

† Mineral premix (g/kg): 314.0 g CaCO₃; 469.3 g KH₂PO₄; 147.4 g MgSO₄·7H₂O; 49.8 g NaCl; 10.9 g Fe (II) gluconate; 3.12 g MnSO₄·H₂O; 4.67 g ZnSO₄·7H₂O; 0.62 g CuSO₄·5H₂O; 0.16 g KI; 0.08 g CoCl₂·6H₂O; 0.06 g NH₄ molybdate; 0.02 g NaSeO₃.

water was added to made stiff dough. The mixed ingredients were finally made to expanded pellets with 0.35–1 mm diameter, which were produced by using a double-helix plodder (F-26, SCUT industrial factory). The experimental diets were stored at –20°C until the usage for the feeding experiment.

For the second experiment, during the acclimation period, the fish were fed a commercial diet (protein 52%, lipid 8%) (Shandong Shengsuo Fishery Culture Feed Research Center, Co., Ltd) for 2 weeks. After that, 180 zebrafish with initial weight 0.315 ± 0.005 g were randomly allocated to two treatments: Control and HSL-IN-1 (three replicates per treatment, thirty fish per replicate). HSL-IN-1 (HY-101509, MedChemExpress (MCE)), a potent and orally active HSL inhibitor, was dissolved in dimethyl sulfoxide. Wheat flour dough can be solidified by mixing wheat flour and suitable amount of water. In experiments, we mixed the wheat flour and inhibitor and added 20% water to make a dough. Then we used household mini grinder (Yongkang Tianqi Shengshi Industry and Trade Co., Ltd) to ground the dough into small-size particles. Afterwards, we screened the particles to obtain wheat flour dough in the size of sixteen meshes to twenty meshes (0.83–1 mm), which is the suitable size for adult zebrafish to eat according to our previous experiment^(45,46). The diet for the HSL-IN-1 group contained 80 mg/kg of HSL-IN-1. Each morning, dough particles at 1% of body weight, containing HSL-IN-1 or not, were fed to fish in different groups, respectively. Afterwards, the fish in both treatments were fed with the basic diet at 3% of their body weight with two times per d (10.00 and 18.00) for 5 weeks.

In both feeding experiments, the weight of all fish in each tank was recorded every week, and the feeding amount was adjusted accordingly. At the end of the feeding trial, all fish was fasted for 12 h, then the whole body, liver, muscle, and blood samples were collected and frozen immediately for further analysis.

Behaviour analyses and oxygen consumption rate

Movement behaviour was recorded by using an automated live video-tracking system (ZebraLab software; ViewPoint Life Sciences), as described in our previous study⁽⁴⁵⁾. The camera was calibrated to detect infrared light and was set to 25 frames per second. During the tracking, fish were illuminated with both infrared light and white light with 75 lux in the ZebraCube for 24 h (light/dark, 14 h/10 h). The integration period (the time intervals used to measure distance swum in each experiment) was 2 min for experimental animal. The swimming activity level was evaluated by calculating the total movement length (mm) during each video recording period. The OCR was measured as described previously⁽⁴⁶⁾. After being starved for 24 h, twelve zebrafish from each type (n 12) were weighed and then separately transferred into a chamber that contained 0.66 litres of fresh water. The OCR was gauged by standard polarographic techniques using a Clark-type Oxygen Meter (SI Strathkelvin Instruments Oxygen Meter, Model 782, plus Mitocell MT 200) at 28°C after 1 h of enclosure within the chamber. The OCR was expressed as micrograms of O₂ consumed per minute per gram of body weight.

Biochemical analyses

The samples were weighed and homogenised on ice in nine volumes (v/w) of PBS (1×) and then centrifuged at 2500 × g at 4°C for 30 min. The supernatant was collected and stored at –80°C until analysis. The concentrations of TAG (glycerophosphate oxidase – peroxidase (GPO-PAP) method, 510 nm), NEFA (acetyl coenzyme A synthase – acetyl coenzyme A oxidase – peroxidase (ACS-ACOD-POD) method, 546 nm) NEFA, glycogen (anthrone colorimetry, 620 nm), lactate (lactate dehydrogenase – 5-methylphenazinium methosulfate – nitroblue tetrazolium (LDH-PMS-NBT) method, 530 nm) and pyruvate (pyruvate oxidase method, 505 nm) in tissue were measured using LabAssay kits (Cat. No. A110–1, A042–2, A043–1, A019–2 and A081–1, Jiancheng Biotech Co.), respectively, according to the manufacturer's instructions. The total protein content of whole body (six fish from each treatment, n 6) was measured by the Kjeldahl method after acid digestion using a 2300 Kjeltac Analyzer Unit (FOSS Tecator). The total lipid content of whole body (six fish from each treatment, n 6) was evaluated by extracting lipid using chloroform/methanol (2:1, v/v) according to the method previously described⁽⁴⁷⁾. The extracted lipid was used for the subsequent analysis of lipid composition. The lipid samples (six samples per treatment) dissolved in chloroform were pointed on Silica Gel TLC plates (200 mm × 200 mm). Firstly, a solvent system consisting of 0.25% KCl/methanol/isopropyl acid chloroform/methyl acetate (9/10/25/25/25 by volume) was used to isolate the polar lipids for 100 min. Then, another solvent system consisting acetic acid/ether/isohexane (1.5/25/80 by



Table 2. Primer sequences for qRT-PCR analysis in zebrafish

Gene name	Sequences (5' to 3')	GenBank NO.
Genotyping		
<i>hsla</i>	F: CGTCTGTTGGGGTTCATGAAG R: CCTGGGTCTGTTTCATCCAAA	NC_007130-7
Lipolysis-related		
<i>atgl</i>	F: ACACACTTACACCGCGTGAT R: AGCACGTTTTCTCCATCCCGT	NC_007136-7
<i>hslb</i>	F: TGTTTGAGGAAGATGGCGACT R: CTGCCTTGGTGTCCATCACTA	NC_007127-7
FAO-related genes		
<i>pparaa</i>	F: TGCTGGACTACCAGAAGTGTGACA R: TGCTGGCTGAGAACACTTCTGAG	XM_005164753-4
<i>cpt1aa</i>	F: CATCCTTAGGCCTGCTTCCAAA R: ACCATGACACCCCAACTAACAT	NM_001044854
<i>acox1</i>	F: TGGAAGGACATGATGCGCTTT R: AGGCTGCCGGGCAAAA	NM_213147-1
Lipogenesis-related genes		
<i>srebf1c</i>	F: ACGCCTGTTGTTGTTGTTGT R: GTCCAGAGTGTCCAGAGAAGT	NM_001105129-1
<i>acc</i>	F: GCGTGGCCGAAACATGGCAG R: GCAGGTCCAGCTTCCCTGCG	NC_007116-7
<i>fasn</i>	F: GGAGCAGGCTGCCTGTGTC R: TTGCGCCTGTCCCACTCCT	XM_009306806-1
<i>dgat2</i>	F: ACGCATAACCTGCTTCCC R: TCCTGTGGCTTCTGTCCC	NM_001030196-1
Glucose uptake-related genes		
<i>glut2</i>	F: CAGCCTGTGTATGCCACTATCG R: CCGCTCTGTCCACCATCAAC	DQ098687-1
Glycolysis-related genes		
<i>gck4</i>	F: ACGAGAAGCTGATTGGTGGG R: TCTGGGAGACAAAGCGTGT	NM_001045385-2
<i>pk (liver)</i>	F: ATCACTGCCCGCAACACCA R: TCATTCCTGCTTCCACCATCTCC	NM_201289-1
<i>pk (muscle)</i>	F: TGAACATCGCTGCATGAACTT R: TCAAAGCTGGCACAAAGCTTCA	NM_199333-1
<i>pfk (liver)</i>	F: GTAACACGCATGGCATTTTTG R: TCGCCAGTTTGTATGTATCTCCT	NM_001017596
<i>pfk (muscle)</i>	F: ATCACATCCGCTCTGATCATGG R: TGGTCTGGAAATCCTTACAGCG	NM_001004575
<i>pdha1a</i>	F: CAGGAACGGTGCCAGGATTG R: GCCTCATGGTCTGCATTGTTCT	NC_007116-7
Glycogen phosphorylase-related genes		
<i>pygma</i>	F: GGGTGCACCTTGCAGAACCA R: CAGCAAGACGACCAAGACCT	NC_007132-7
<i>pygmb</i>	F: CATCACTGTGCGTACTTTCG R: AGATGATTTCCAGGTGGCGG	NC_007118-7
<i>pyg(L)</i>	F: GGAGAATGTGGCCGAGCTAA R: CAGAAGCTGCTGTGCGGAT	NC_007124-7
Protein breakdown-related genes		
<i>apn</i>	F: GGTGGCTTTTACCGGAGTGAATA R: CAAGGAATGCTTTTCTGGCCTC	XM_001920383-5
<i>bckdha</i>	F: TCCGACGAGAAGCCGCGATT R: GCCCTGTCTGTCCATCACTCTG	NM_001024419-1
<i>glud1a</i>	F: AGGACATTGTGATTCGGGATT R: CCTCAGATCCAGCCCAAGGTTAT	NM_212576
<i>bcat2</i>	F: CCGACCATCGCTGTCCAGAATG R: TCATGGTGCCGACCTCAGTGAT	NM_001002676-2
<i>asns</i>	F: CAGAAGACTGACAGCGTGGTGA R: GGTGTGGAGCCTTGTGGAAGT	NM_201163-3
Protein synthesis-related genes		
<i>mtor</i>	F: TGGGAGCAGACAGGAATGAAGG R: TGCACCTGCTGAAAAGAAGT	NM_001077211-2
Inflammation and apoptosis-related genes		
<i>cas3</i>	F: GAGACCGTGTCCCATCACT R: GCATCCTTTCACGACCATCTG	NC_007112-7
<i>cas8</i>	F: CATCATGCTTCAATGGGTGCT R: CGCTTCTCGGATTTCAACTGG	NC_007117-7 NC_007134-7
<i>cas9</i>	F: AGTACCACTGAGACCTGAA R: GGCATCCATCTGTAGCA	
<i>il1β</i>	F: CTCAGCCTGTGTGTTGGGA R: GGGACATTTGACGGACTCG	NC_007121-7
<i>il8</i>	F: AAGCCGACGCATTGGAAGAAC R: GTTGTCAATCAAGGTGGCAATGA	NC_007112-7

Table 2. (Continued)

Gene name	Sequences (5' to 3')	GenBank NO.
<i>il10</i>	F: CGGGATATGGTGAATGCAAGA R: AGAGCAAATCAAGCTCCCC	NC_007122-7
<i>il12a</i>	F: CACCGATTTCCAACGCCAAG R: TGACTTGGAAAGGGGCGATTG	NC_007126-7
Reference genes		
<i>ef1a</i>	F: CCCCTGGACACAGAGACTTCATC R: ATACCAGCCTCAAACCTCACCGAC	L23807-1
<i>β-actin</i>	F: GTCATCACCATCGGCAAT R: CGTGGATACCGCAAGATT	AY222742

volume) was used to isolate the natural lipids for 150 min. Subsequently, all the TLC plates were put in an oven at 50°C for 30 min and then dyed with iodine for 20 min. The separated TAG, DG, MG and phospholipids from the whole body was quantified by TLC scanner (Kezhe KH-3000) at room temperature according our previous method⁽⁴⁶⁾.

Histological H&E, Nile Red and PAS staining

Neutral lipid accumulation was visualised using Nile Red staining in live zebrafish, as shown in our previous study⁽⁴⁶⁾. Nile Red (N3013; Sigma) was dissolved in acetone at 2 mg/ml as the stock solution. Three fish from each treatment were dyed in water containing 0.1 mg/ml Nile Red for 5 h at 28°C in a lightproof environment. After that, the fish were washed in the tank containing fresh water for five times, at 30 min intervals. At last, the fish were anaesthetised with MS-222 (17 mg/l) (tricaine methanesulfonate, Sigma-Aldrich) and photographed by using an Olympus SZX16 FL stereomicroscope (Olympus) at an excitation wavelength of 488 nm. Six pieces of fish livers and intestines from each treatment were fixed in 4% paraformaldehyde solution and then embedded in paraffin. Sections of 5-µm thickness were used for the subsequent staining of Harris's hematoxylin–eosin mixture (H&E) and periodic acid Schiff⁽⁴⁸⁾ staining as depicted in our previous study⁽³⁶⁾.

Quantitative real-time PCR

Total RNA from liver, muscle and viscera tissues was extracted by using a TriPureReagent (Aidlab) for subsequent cDNA synthesis according to the manufacturer's protocol. The quality of RNA and cDNA was tested by a NANODROP 2000 Spectrophotometer (Thermo) as described previously⁽⁴⁹⁾. The genes of elongation factor 1α and (*ef1a*) and β-actin were used as the housekeeping gene controls for the normalisation of gene expression. The qPCR reaction consisted of 95°C for 10 min, 40 cycles of 95°C for 5 s and 60°C for 18 s. The primers for qPCR were designed to overlap an intron by using the National Center for Biotechnology Information (NCBI) website and synthesised by Ruimian Biological Technology Co., Ltd (Shanghai, China). The melting curves of amplified products were generated to ensure the specificity of assays at the end of each PCR. The qPCR efficiency was between 97% and 104%, and the correlation coefficient was over 0.97 for each gene. The qPCR was conducted by using the 2^{-ΔΔCt} method according to our previous research⁽³³⁾. All the primer sequences for qRT-PCR analysis are shown in Table 2.

Western blotting

The muscle tissues from each genotype (three pooled samples per assay, one sample was mixed with tissues from three fish, about 50 mg) were used for the western blot analysis. Muscle homogenates were prepared by using the RIPA lysis buffer (Beyotime Biotechnology) for western blot analysis. Proteins were separated by using 8% or 12% sodium dodecyl sulphate-polyacrylamide gel electrophoresis (SDS-PAGE) and transferred electrophoretically to nitrocellulose membranes. Membranes were incubated for 1 h in a blocking solution containing 5% bovine serum albumin in a mixture of TRIS-buffered saline (TBS) and polysorbate 20 (TBST). Membranes were washed briefly in a mixture of TBST and incubated overnight at 4°C with the anti-mTOR (1:800, #2972, CST), anti-GAPDH (1:3000, AB0036, Abways) and anti-A-tubulin (1:3000, M1501-1, HuaBio) antibodies. Afterwards, the blots were washed to remove excessive primary antibody binding and finally were incubated for 1 h with horseradish peroxidase-conjugated secondary antibody. The western blot images were obtained by using the Odyssey CLx Imager (Licor).

Statistical analyses

Independent-samples *t* test was performed to evaluate the significant differences among measured variables ($P < 0.05$). All data were conducted using the SPSS Statistics 28.0 software (IBM). Figures were generated using GraphPad Prism version 6.1 (<https://www.graphpad.com/scientific-software/prism/>, GraphPad Software Inc.).

Results

The effect of impaired Hsl function on growth and exercise activity

In the 5-week feeding trial, the *hsla*^{-/-} zebrafish showed retarded growth (Fig. 1(a)) and markedly lower final body weight (Fig. 1(b)) but demonstrated significantly higher condition factor (Fig. 1(c)) when compared with the WT fish. However, there were no differences in growth (Fig. 1(f)) and final body weight (Fig. 1(g)) between the control and HSL-IN-1-treated groups, but the HSL-IN-1-treated fish showed markedly higher viscerosomatic index (VSI) (Fig. 1(h)) than the control group. Compared with their WT siblings, *hsla*^{-/-} zebrafish showed a lower respiration rate (Fig. 1(e)), but there was no difference in the swimming activity, which was measured by swimming distance during the assay period (Fig. 1(d)), between the two genotypes. Accordingly, the HSL-IN-1-treated group also showed a significantly lower respiration rate (Fig. 1(j)) than the control group, but there was no difference in the swimming activity (Fig. 1(i)) between the two treatments.

Impaired Hsl function caused lipid accumulation

The *hsla*^{-/-} zebrafish exhibited more abdominal fat deposition (Fig. 2(a)) and had visible white adipose tissue (Fig. 2(b)) in viscera than WT fish. Correspondingly, the HSL-IN-1-treated fish also showed more abdominal fat deposition (Fig. 2(i)) and had visible adipose tissue (Fig. 2(j)) in viscera compared with

the control group. These are representative results of the treatment (Fig. 2(a),(b),(i),(j)). Furthermore, the *hsla*^{-/-} zebrafish had markedly higher TAG contents in whole body, muscle, liver and viscera (Fig. 2(c)–(e) and (g)), and significantly higher levels of FFA in the liver and visceral tissue (Fig. 2(f) and (h)). The whole-body lipid was remarkably increased in the fish fed with HSL-IN-1 treatment compared with the control group (Fig. 2(k)). Accordingly, significantly higher TAG content was found in the muscle, liver and viscera in the HSL-IN-1-treated fish than in the control group (Fig. 2(l), (m) and (o)). The HSL-IN-1-treated fish showed higher FFA content in liver but lower that in viscera compared with control group (Fig. 2(o)–(p)).

The effect of impaired Hsl function on gene expressions of lipid metabolism

Compared with the WT fish, the *hsla*^{-/-} zebrafish showed lower expression of *atgl*, *hsla*, *hslb* and *cpt1aa*, and higher expression of *pparaa* in liver (Fig. 3(a)), and lower expression of *atgl*, *hsla*, *hslb*, *pparab*, *cpt1aa* and *acox1* in muscle (Fig. 3(b)), whereas in viscera, it demonstrated lower expression of *hsla*, *atgl*, *cpt1aa*, and *acox1*, and higher expression of *pparaa* (Fig. 3(c)). These genes were associated with the process of lipolysis and fatty acid oxidation. Similarly, the HSL-IN-1-treated fish exhibited lower expression of *atgl*, *hsla*, *pparaa*, and *cpt1aa* in liver (Fig. 3(e)), but there was no difference between HSL-IN-1 treatment and control groups in the expression of genes related to lipolysis and fatty acid oxidation, including *atgl*, *hsla*, *pparaa*, *cpt1aa*, and *acox1* either in muscle or viscera (Fig. 3(f) and (g)). The expression of key lipogenesis-related genes such as *srebp1c*, *acc*, *fasn* and *dgat1a* was markedly increased in the liver of *hsla*-mutant zebrafish compared with WT fish (Fig. 3(d)). However, the fish treated with HSL-IN-1 showed significantly lower expression of *acc*, *fasn* and *dgat1a* than the control group (Fig. 3(h)).

Impaired Hsl function changed lipid profile of whole body

The proportion of different lipid classes present in whole body was changed by *hsla*^{-/-} or HSL-IN-1 treatment. In the *hsla*^{-/-} zebrafish, the percentages of TAG and DG were increased significantly compared with WT fish, while the proportions of MG and phospholipids were significantly reduced (Fig. 4(a)–(e)). Besides, in these changes between the *hsla*^{-/-} zebrafish and WT fish, phospholipids contributed the greatest part (46.57% *v.* 37.52%) (Fig. 4(a)). In the HSL-IN-1-treated fish, the percentages of DG, MG and phospholipids were reduced markedly compared with the control group, while only the proportion of TAG was significantly increased (Fig. 4(f)–(j)). Besides, in these changes between the HSL-IN-1 treatment and control group, TAG contributed the greatest proportion of the total lipids (50.57% *v.* 62.85%) (Fig. 4(f)).

The effect of impaired Hsl function on carbohydrate metabolism

The *hsla*^{-/-} zebrafish exhibited markedly lower content of glycogen in liver and muscle than WT fish (Fig. 5(a) and (b)). Accordingly, the pyruvate concentration in the muscle of *hsla*^{-/-}



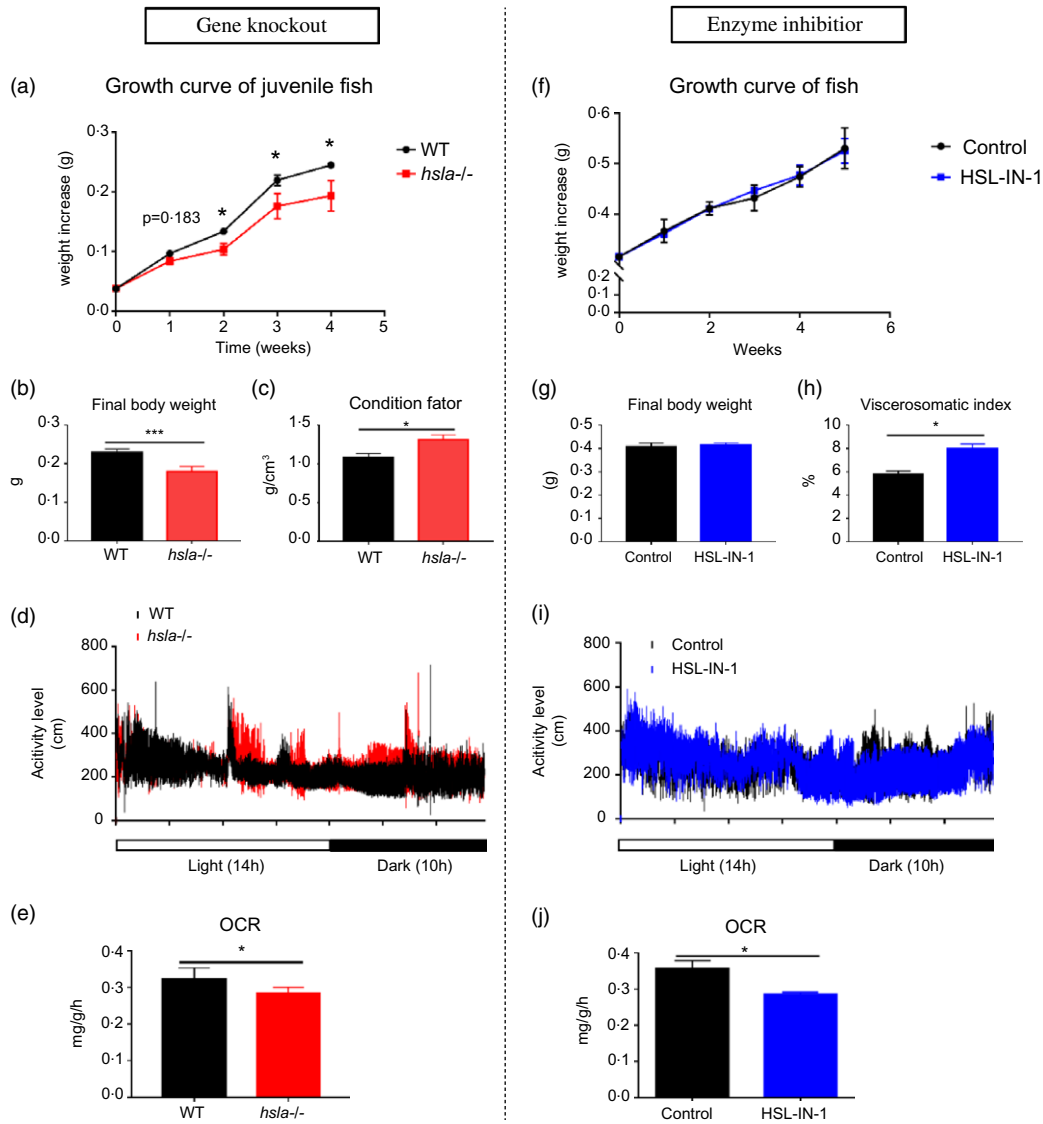


Fig. 1. The effect of impaired Hsl function on growth and exercise activity. WT and *hsla*^{-/-} fish: (a) growth curve of; (b) final body weight; (c) condition factor (% = 100 × final fish weight/(final fish length)³); (d) swimming activity (*n* 6); (e) the OCR was calculated as OCR = (ΔO₂ concentration (μg/l) × water volume (l))/(fish weight (g) × time (min)). Control and HSL-IN-1-treated fish: (f) growth curve; (g) final body weight; (h) viscerosomatic index: visceral weight/body weight × 100 %; (i) swimming activity; (j) OCR. All data are presented as mean ± SEM. **P* ≤ 0.05, ***P* ≤ 0.01, ****P* ≤ 0.001.

zebrafish was significantly increased compared with the control group, but there was no difference in the concentration of lactate in muscle between two genotypes (Fig. 5(c) and (d)). Consistently with this, the expressions of gene-related glycogen phosphorylase were markedly increased in *hsla*^{-/-} zebrafish, including *pyg(L)* in liver and *pygmb* in muscle, compared with WT fish (Fig. 5(e) and (f)). In the genes related to glucose transport and glycolysis, the *hsla*^{-/-} zebrafish showed higher expression of *gck4*, *pfk*, *pk* and lower expression of *glut2* in liver, and higher expression of *glut2* and *pk* in muscle than WT fish (Fig. 5(g) and (h)). The fish treated with HSL-IN-1 showed significantly higher glycogen content in liver but significantly lower glycogen content in muscle than the control group (Fig. 5(i) and (j)). Furthermore, the content of lactate in muscle of HSL-IN-1 group was markedly increased compared with the control group (Fig. 5(k)). Consistently with this, the expression of *pyg(L)*

in liver was markedly reduced, but the expression of *pygmb* was significantly increased in the muscle of fish treated with HSL-IN-1 compared with the control group (Fig. 5(l) and (m)). The fish treated with HSL-IN-1 exhibited higher expression of *gck4* and lower expression of *glut2*, *pfk*, *pk*, and *pdha1a* in liver, along with higher expression of *glut2*, *pfk*, *pk*, and *pdha1a* in muscle, as compared with the control group (Fig. 5(n) and (o)).

The effect of impaired Hsl function on protein metabolism

The *hsla*^{-/-} zebrafish showed significantly lower whole-body protein content than their WT siblings (Fig. 6(a)). Among genes related to protein or amino acid breakdown, the expression of *apn* was increased markedly in the *hsla*^{-/-} zebrafish, but there was no difference in the expressions of *bckdha*, *bca2* and *mtor*

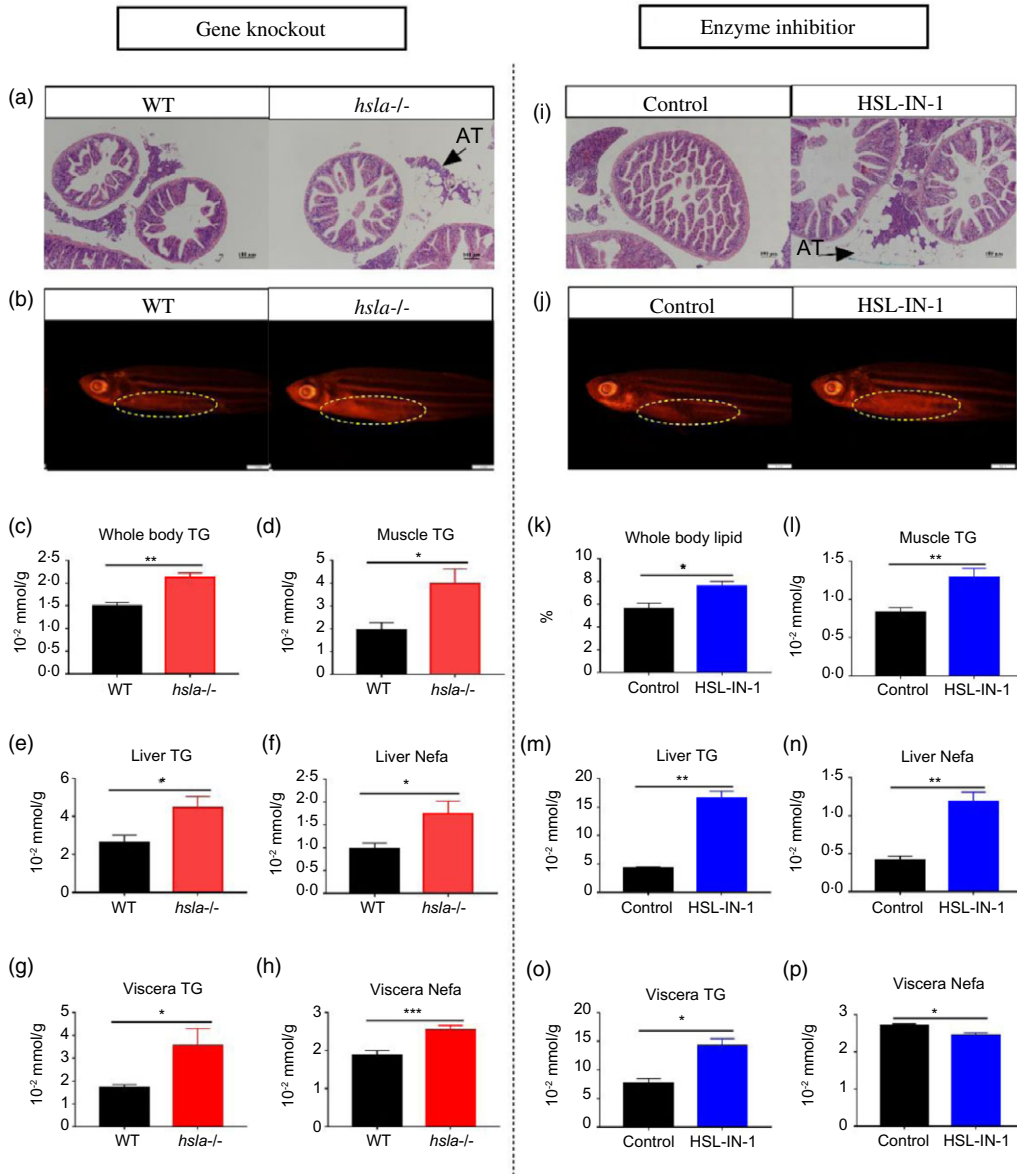


Fig. 2. Impaired Hsl function caused lipid accumulation. WT and *hsla*^{-/-} fish: (a) H&E staining of intestine and attached adipose tissue, scale bars, 100 μm; (b) pictures taken after Nile Red staining, scale bars, 2 mm; (c) the total TAG content in whole-body fish; (d) TAG content in muscle; (e) TAG content in liver; (f) non-essential fatty acid (NEFA) content in liver; (g) TAG content in viscera; (h) NEFA content in viscera. Control and HSL-IN-1-treated fish: (i) H&E staining of intestine and attached adipose tissue, scale bars, 100 μm; (j) pictures taken after Nile Red staining, scale bars, 2 mm; (k) the total lipid content in whole-body fish; (l) TAG content in muscle; (m) TAG content in liver; (n) NEFA content in liver; (o) TAG content in viscera; and (p) NEFA content in viscera. All data are presented as mean ± SEM. **P* ≤ 0.05, ***P* ≤ 0.01, ****P* ≤ 0.001. H&E, hematoxylin–eosin.

between two genotypes (Fig. 6(b)). Moreover, the *hsla*^{-/-} zebrafish showed lower expression of T-mTOR protein, which is essential for protein synthesis, than WT fish (Fig. 6(c) and (d)). The content of whole-body protein was significantly reduced in the fish treated with HSL-IN-1 compared with the control group (Fig. 6(e)). The fish treated with HSL-IN-1 showed higher expression of *apn* and *glud1a* and lower expression of *bca2* in muscle than the control group (Fig. 6(f)). Furthermore, the expression of T-mTOR protein in HSL-IN-1-treated fish tended to reduce as compared with the control group (Fig. 6(g) and (h)).

The effect of impaired Hsl function on the inflammation and apoptosis

The *hsla*^{-/-} zebrafish exhibited higher expression of *cas3*, *cas8*, *il1β* and *il8* in liver, while expressed higher *cas9*, *il1β* and *il8* in muscle than their WT siblings (Fig. 7(a) and (b)). Similarly, the fish treated with HSL-IN-1 showed higher expression of *cas3*, *il10* and *il12a* in liver, while expressed higher *cas9*, *il10* and *il12a* in muscle compared with the control group (Fig. 7(c) and (d)). The genes mentioned above are all associated with inflammation and apoptosis.

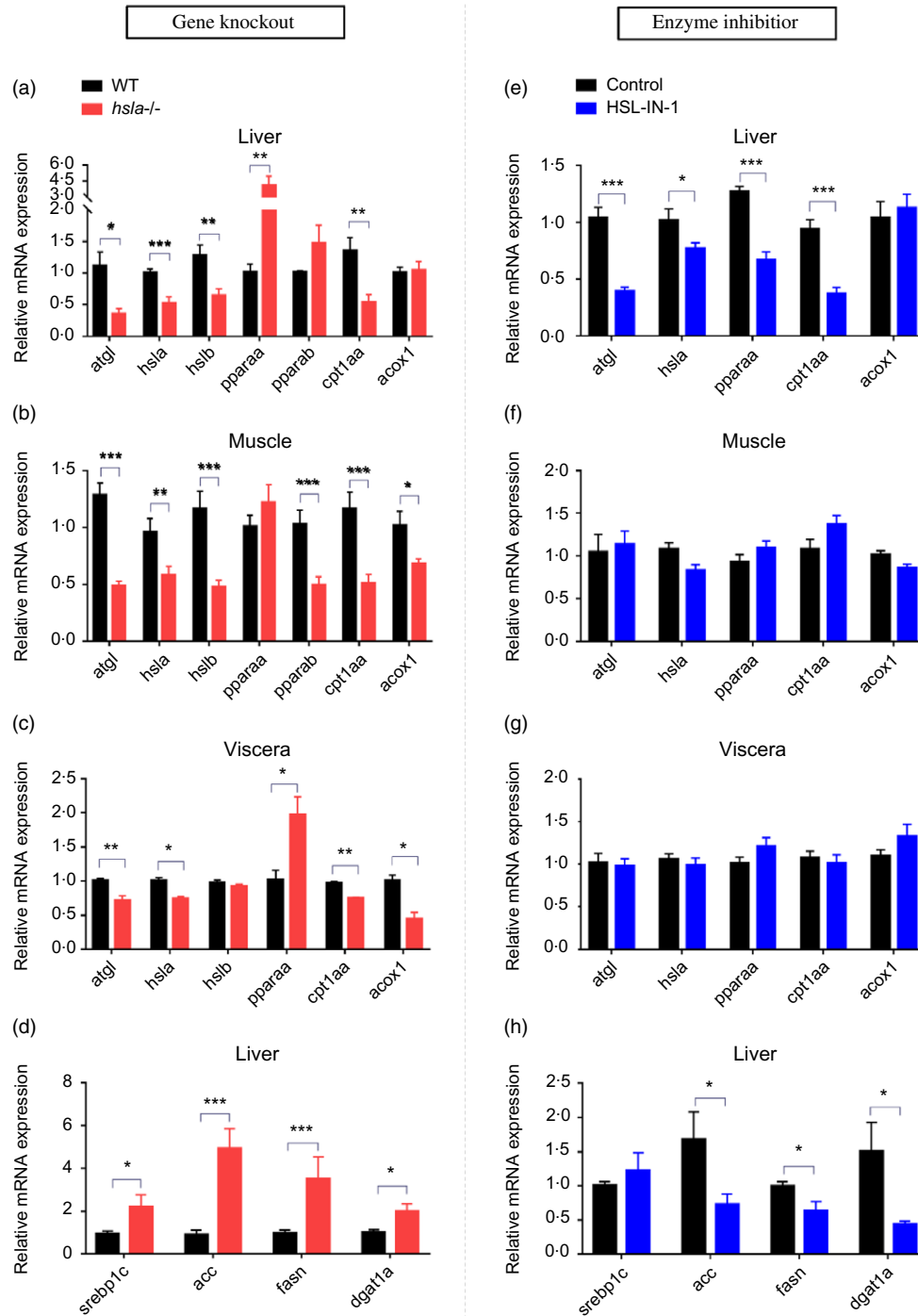


Fig. 3. The effect of impaired Hsl function on gene expressions of lipid metabolism. WT and *hsla*^{-/-} fish: (a) the expression of lipolysis and fatty acid oxidative (FAO)-related genes in fish liver (*n* 6); (b) the expression of lipolysis and FAO-related genes in fish liver (*n* 6); (c) the expression of lipolysis- and FAO-related genes in fish liver (*n* 6); (d) the expression of lipogenesis-related genes in fish liver (*n* 6). Control and HSL-IN-1-treated fish: (e) the expression of lipolysis- and FAO-related genes in fish liver (*n* 6); (f) the expression of lipolysis- and FAO-related genes in fish liver (*n* 6); (g) the expression of lipolysis- and FAO-related genes in fish liver (*n* 6); (h) the expression of lipogenesis-related genes in fish liver (*n* 6). All data are presented as mean \pm SEM. **P* \leq 0.05, ***P* \leq 0.01, ****P* \leq 0.001. *atgl*, adipose triglyceride lipase; *hsla*, hormone-sensitive lipase a; *hslb*, hormone-sensitive lipase b; *pparaa*, peroxisome proliferator-activated receptor α ; *pparab*, peroxisome proliferator-activated receptor β ; *cpt1aa*, carnitine palmitoyl transferase 1a; *acox1*, acyl-CoA oxidase 1; *srebp1c*, sterol regulatory element-binding transcription factor 1c; *acc*, acetyl-CoA carboxylase; *fasn*, fatty acid synthase; *dgat1a*, diglyceride acyltransferase 1a.

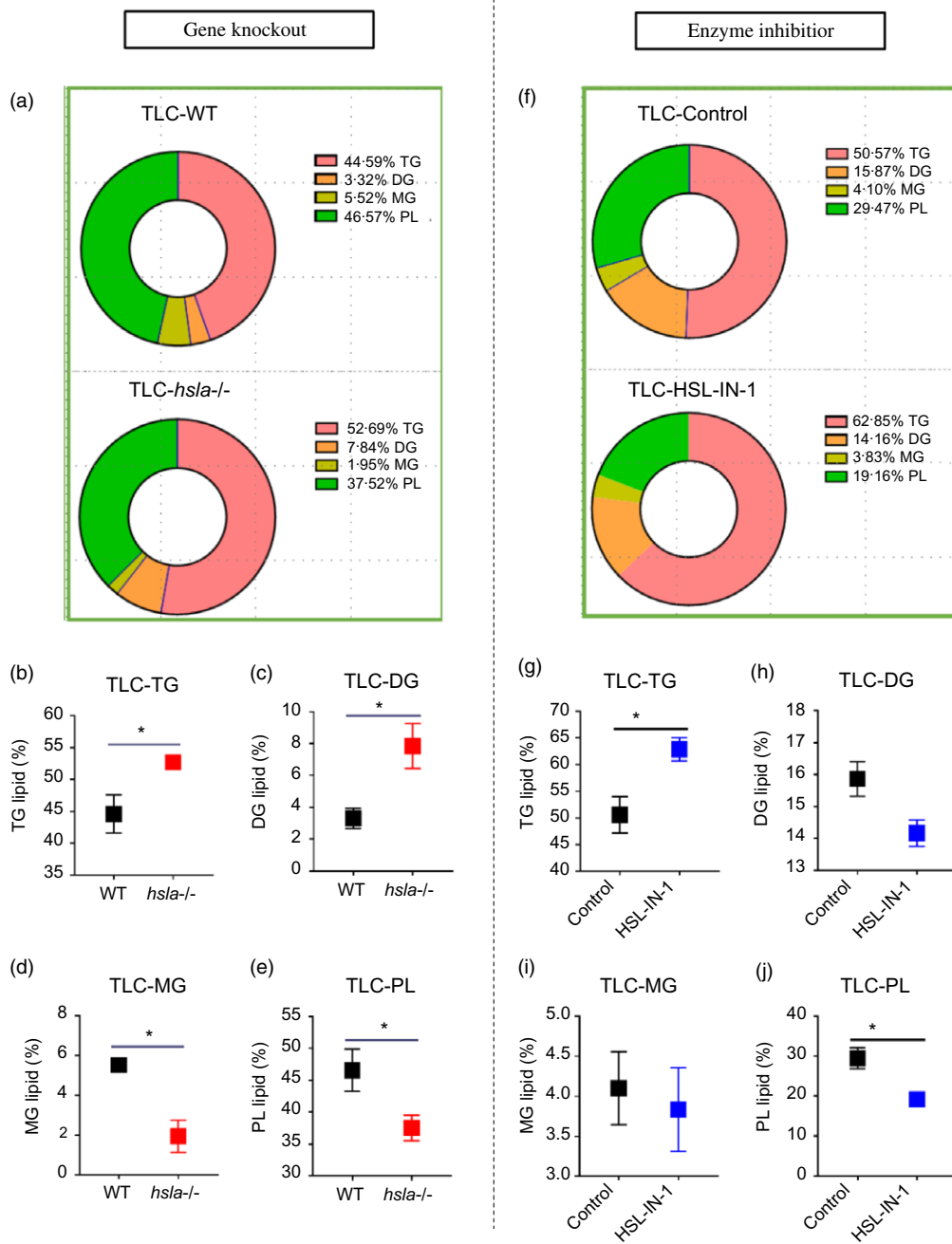


Fig. 4. Impaired Hsl function changed lipid profile of whole body. WT and *hsla*^{-/-} fish: (a) the average proportion of lipid class composition; (b) the percentage of TAG to total lipid (*n* 8); (c) the percentage of diacylglycerol (DG) to total lipid (*n* 8); (d) the percentage of monoglyceride (MG) to total lipid (*n* 8); (e) the percentage of phospholipid (PL) to total lipid (*n* 8). Control and HSL-IN-1-treated fish: (f) the average proportion of lipid class composition; (g) the percentage of TAG to total lipid (*n* 8); (h) the percentage of DG to total lipid (*n* 8); (i) the percentage of MG to total lipid (*n* 8); (j) the percentage of PL to total lipid (*n* 8). All data are presented as mean ± SEM. **P* ≤ 0.05, ***P* ≤ 0.01, ****P* ≤ 0.001.

Discussion

The effect of impaired Hsl function on growth and exercise activity

Normal metabolic homeostasis is essential for the growth of living organisms⁽⁵⁰⁾. Lipolysis plays a key role in the mobilisation of energy from fat sources such as TAG. Therefore, as a rate-limiting enzyme in the process of lipolysis, we hypothesised that the impaired function of Hsl would have an impact on the growth

of zebrafish. In the present study, the *hsla*^{-/-} zebrafish showed a significant decline in growth. Similar to our result, in the other zebrafish model with defective lipolysis, the *atgl*-deficient fish also exhibited significant growth retardation⁽⁴⁵⁾. In mammals, the eight-month-old mice with global or specific-adipocyte *Hsl*-knockout both developed a lower weight gain than the WT group⁽²²⁾. Therefore, Hsl inhibition might reduce growth through disturbing energy metabolism. In animal trials, the OCR is a visible indicator to describe the basal respiration,

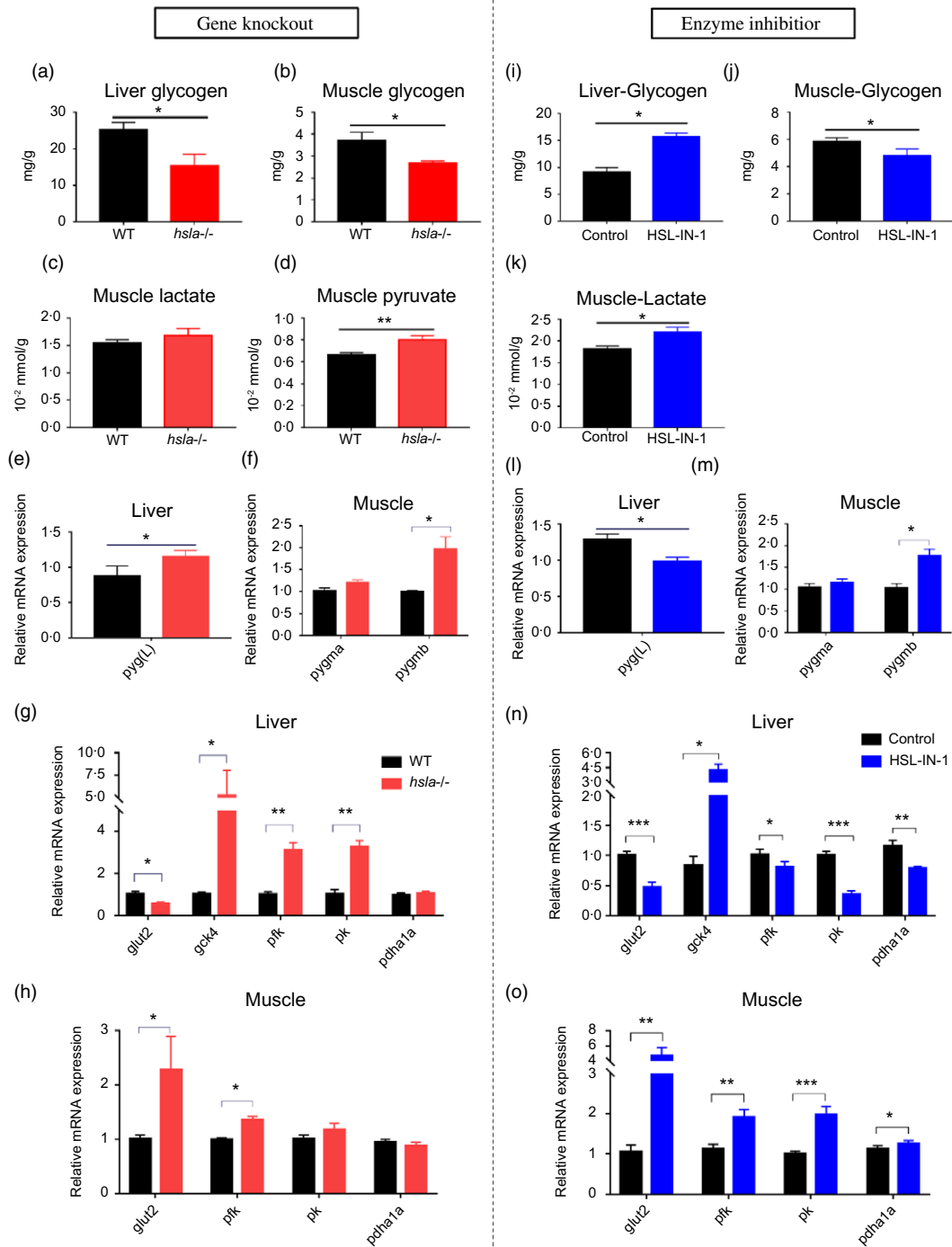


Fig. 5. The effect of impaired Hsl function on carbohydrate metabolism. WT and *hsla*^{-/-} fish: (A) the content of glycogen in liver; (b) the content of glycogen in muscle; (c) the content of lactate in muscle; (d) the content of pyruvate in muscle; (e) the expression of glycogen phosphorylase-related genes in liver; (f) the expression of glycogen phosphorylase-related genes in liver; (g) the expression of glucose transport and glycolysis-related genes in liver; (h) the expression of glucose transport and glycolysis-related genes in muscle. Control and HSL-IN-1-treated fish: (i) the content of glycogen in liver; (j) the content of glycogen in muscle; (k) the content of lactate in muscle; (l) the expression of glycogen phosphorylase-related genes in liver; (m) the expression of glycogen phosphorylase-related genes in muscle; (n) the expression of glucose transport and glycolysis-related genes in liver; (o) the expression of glucose transport and glycolysis-related genes in muscle. All data are presented as mean ± SEM. **P* ≤ 0.05, ***P* ≤ 0.01, ****P* ≤ 0.001. *pyg(L)*, glycogen phosphorylase in liver; *pygma*, glycogen phosphorylase muscle a; *pygmb*, glycogen phosphorylase muscle b; *glut2*, glucose transporter 2; *gck4*, glucokinase 4; *pfk*, phosphofructokinase; *pk*, pyruvate kinase; *pdha1a*, pyruvate dehydrogenase E1 subunit alpha 1a.

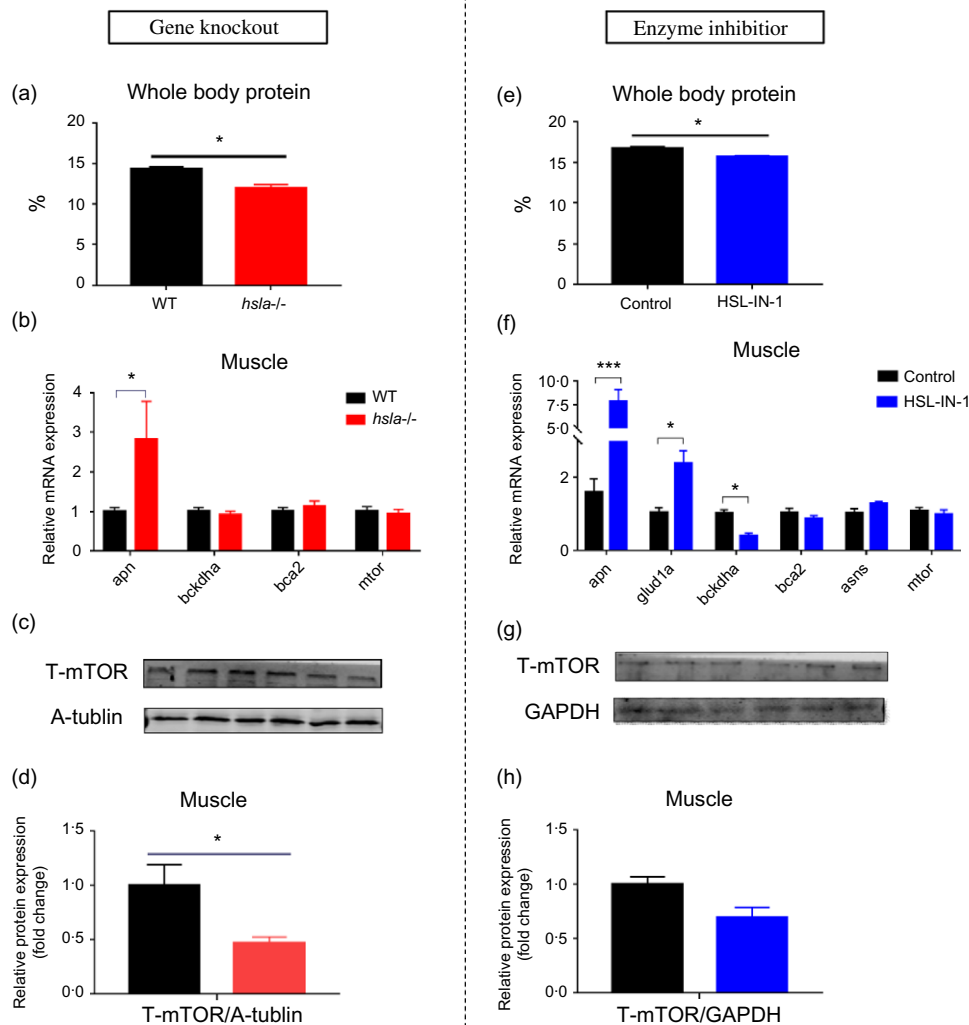


Fig. 6. The effect of impaired Hsl function on protein metabolism. WT and *hsla*^{-/-} fish: (a) the content of protein in whole-body fish; (b) the expression of protein and amino acid metabolism-related genes in muscle;⁽³²⁾ the protein expression of T-mTOR in muscle. Control and HSL-IN-1-treated fish: (e) the content of protein in whole-body fish; (f) the expression of protein and amino acid metabolism-related genes in muscle; (g and h) the protein expression of T-mTOR in muscle. All data are presented as mean ± SEM. **P* ≤ 0.05, ***P* ≤ 0.01, ****P* ≤ 0.001. *apn*, aminopeptidase N; *bckdha*, branched-chain keto acid dehydrogenase E1 subunit α; *bca2*, *asns*, asparagine synthetase; *mtor*, mechanistic target of rapamycin kinase. T-mTOR, total mechanistic target of rapamycin kinase; GAPDH, glyceraldehyde-3-phosphate dehydrogenase.

energy expenditure, ATP production and oxidative capacity of living organisms⁽⁵¹⁾. In the present study, the *hsla*-knockout zebrafish and the HSL-IN-1-treated fish both exhibited a significant decrease in OCR but showed similar movement activity. Horikoshi *et al.*⁽⁵²⁾ showed that when enhancing the utilisation of exogenous fatty acids, the human cardiomyocyte had a higher OCR associated with basal and maximum respirations. Therefore, our results suggest that the decrease in OCR in the *hsla*-knockout zebrafish and HSL-IN-1-treated fish is most likely unrelated to the movement activity. Whether the change of OCR could show more efficient metabolism requires further studies to follow. Interestingly, our results show that the protein accretion in the *hsla*-knockout zebrafish and HSL-IN-1-treated fish were significantly lower than their control groups. Therefore, the decrease in OCR was possibly related to the decreased protein accretion, which is metabolically expensive compared with lipid deposition.

The role of Hsl in lipid metabolism

Disturbances in lipolysis could affect overall lipid homeostasis and thus induce the development of obesity, diabetes and CVD^(1,2). However, the functions of Hsl in the whole-body energy and lipid homeostasis in zebrafish have not been investigated. In our results, we found that the *hsla*^{-/-} and HSL-IN-1-treated zebrafish exhibited (1) more conspicuous intestinal adipose tissue, (2) greater TAG accumulation in different tissues including liver, muscle, and viscera, and (3) reduced expressions of the genes involved in lipolysis and fatty acid oxidation compared with the WT or Control group. These were in agreement with previous studies in the *Hsl*-KO mice and human with mutated *HSL* gene, in which noticeable hepatic steatosis was found^(19,22,24). In addition, the adipose-specific *Hsl*-knockout mice exhibited significant hepatic TAG deposition, impaired lipolytic activity and marked dysregulation of lipid metabolism,

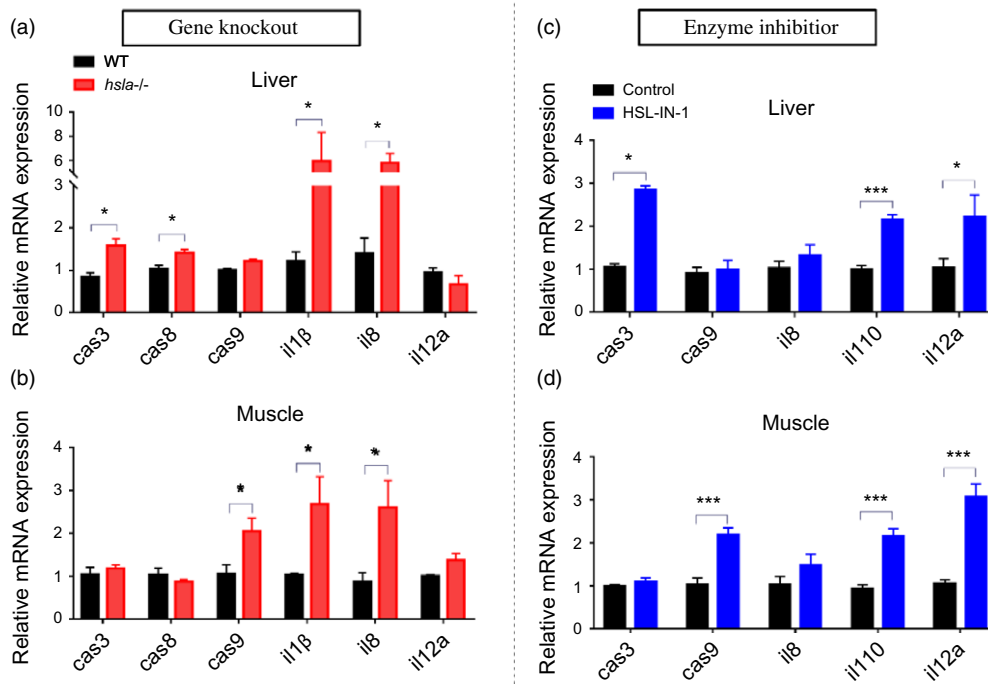


Fig. 7. The effect of impaired Hsl function on the inflammation and apoptosis. WT and *hsla*^{-/-} fish: (a) the expression of inflammation and apoptosis-related genes in liver; (b) the expression of inflammation and apoptosis-related genes in muscle. Control and HSL-IN-1-treated fish: (c) the expression of inflammation and apoptosis-related genes in liver; (d) the expression of inflammation and apoptosis-related genes in muscle. All data are presented as mean \pm SEM. * $P \leq 0.05$, ** $P \leq 0.01$, *** $P \leq 0.001$.

including down-regulation of mRNA levels of genes involved in lipogenesis (*Cebp1a* and *Srebp1c*), lipid uptake (*Cd36* and *Fabp4*) and lipid synthesis (*Fasn* and *Dgat2*)⁽⁵³⁾. As one of the rate-limiting enzymes for lipolysis, ATGL had been reported in many previous studies. The *Atgl* deficiency in mice and human both showed marked hepatic steatosis and severe lipid accumulation in whole body^(54,55). In our previous research, the *atgl*-knockout and *Atgl*-inhibitor-treated zebrafish both exhibited conspicuous lipid accumulation and lipid metabolism disorder^(45,46). Therefore, we could infer that the deficiency of Hsl can weaken the lipolytic activity and the expressions of the genes related to lipid catabolism, leading to lipid accumulation in zebrafish. This was also consistent with the reduction in OCR. In the following TLC assay, we found the *hsla*^{-/-} zebrafish showed higher relative contents of TAG and DG. Considering Hsl has a hydrolytic activity for TAG and DG, our TLC data indicate that the hsl deficiency directly led to the accumulation of TAG and DG. Similarly, for the *Atgl*-inhibitor-treated zebrafish, the TAG content was also markedly increased, indicating that abnormal lipolysis is a major factor in altering lipid profile. All these verified that the Hsl deficiency impairs lipid metabolism, inducing severe lipid accumulation in multiple tissues.

Regulation of Hsl in glucose and protein metabolism

In order to cope with the dynamic nutrient environment, cells need to accurately and dynamically reshape metabolic pathways to maintain energy homeostasis. Therefore, disturbances in lipid metabolism may cause changes in glucose metabolism⁽⁴⁸⁾. In mammals, Park *et al.*⁽⁵⁶⁾ reported that

Hsl-KO mice were protected from diet-induced insulin resistance in heart and skeletal muscle, boosted insulin-stimulated cardiac glucose uptake, and improved the glucose metabolism. Additionally, some previous studies reported that Hsl-inhibitor-treated mice and *Hsl*-deficient mice showed increased glucose tolerance and insulin sensitivity and increased hepatic insulin action^(57,58). Accordingly, the mice lacking adipocyte *Hsl* increased insulin-mediated phosphorylation of AKT^{P-Ser473}, a core protein downstream of the insulin signalling pathway, exhibiting beneficial impacts on systemic glucose homeostasis⁽⁵⁹⁾. In the present study, we found *hsla*^{-/-} zebrafish showed significant glycogen content reductions in both liver and muscle, implying enhanced glycogen utilisation. In addition, *hsla*^{-/-} zebrafish elevated contents of the glucose metabolites, including lactate and pyruvate, in muscle, suggesting that the products of glycogen breakdown were being used for oxidative and energy supply. Consistent with the above biochemical results, the expressions of the genes related to glycogen catabolism (*pygma* and *pyg(L)*) and glycolysis (*glut2*, *gck*, *pfk* and *pk*) were enhanced in *hsla*^{-/-} zebrafish, and a similar gene expression pattern was also observed in the Hsl-inhibitor-treated zebrafish. These data strongly suggested that Hsl deficiency reduces glycogen accumulation and enhances glycogen and glucose utilisation in zebrafish.

Compared with lipid and glucose metabolism, protein metabolism also plays an essential role in energy metabolism and homeostasis. Our finding from the present work showed that *hsla*^{-/-} zebrafish and fish treated with Hsl inhibitor both exhibited a reduction of protein in the whole body. A series

of mammalian and fish studies have reported that the mTOR pathway activates a phosphorylation cascade to accelerate protein synthesis and inhibit proteolysis in muscle^(30,60,61). The present work further indicated that the protein expression of T-mTOR was reduced in the muscle of the *hsla*-knockout and Hsl-inhibitor-treated zebrafish, but the mRNA expression of *apn*, which is related to protein catabolism, was markedly increased. Additionally, our previous study demonstrated that *atgl*-KO zebrafish also showed a significantly lower protein content than their WT siblings⁽⁴⁵⁾. Therefore, the lipolysis disorder due to Hsl deficiency could inhibit the mTOR pathway and enhance the catabolism of protein as an energy source.

Regulation of Hsl in inflammation and apoptosis

Metabolic disorders such as obesity, diabetes, hepatic steatosis and nonalcoholic fatty liver diseases are often accompanied by inflammation and infiltration of immune cells^(62–64). In our present study, the *hsla*^{-/-} and HSL-IN-1-treated zebrafish showed visible fat accumulation and abnormal lipid metabolism. The present work further indicated that the *hsla*^{-/-} and HSL-IN-1-treated zebrafish showed higher expressions of the genes related to inflammation and apoptosis, including *cas3*, *cas8*, *cas9*, *il1 β* , *il8*, *il10*, and *il12a* in liver and muscle. In mammal, the global *Hsl*-KO and adipose *Hsl*-KO mice both exhibited macrophage infiltration in adipose tissues and systemic inflammation, accompanied with the higher expressions of inflammation-related genes, including *Tnfa*, *Il6*, *INOS*, *Cxcl9*, and *Cxcl10*^(22,65). A previous study reported that the mice lacking *Hsl* specifically in adipose tissue showed increased hepatic lipid accumulation and the mRNA expressions of immune cell markers (*Dd11c* and *F4/80*). Hepatic steatosis has been reported to cause the recruitment of inflammasome and activate the immunity and inflammation to develop fibrosis and cirrhosis in liver^(66,67). In addition, excessive lipid deposition in hepatocytes of mice would also induce oxidative stress and increased level of lipopolysaccharide, which can be recognised by Toll-like receptor 4 (TLR4), the macrophage marker that activates downstream signalling pathways to increase inflammatory cytokine production like *Il1 β* , *Il8*, *Il10* and *Tnfa*^(68,69). Therefore, our present study demonstrated that the Hsl inhibition-caused lipid accumulation possibly induced the recruitment of inflammasome or lipopolysaccharide to activate the expressions of the downstream genes related to inflammation and apoptosis. Considering the biological function of HSL, the phenotype of lipid deposition should be mainly caused by the impaired function of HSL. In addition, a lot of studies have proved that lipid accumulation could cause inflammation^(66–69). It should be pointed out that the knowledge about the direct connection between Hsl and inflammation or apoptosis has not been established. Therefore, whether the Hsl could directly regulate inflammation and/or apoptosis still requires further studies.

The differences between gene-knockout and enzymic inhibition models

In the present study, we used gene-knockout and enzymic inhibition, respectively, to study the regulatory functions of Hsl in

nutrient metabolism in fish. Although most phenotypes were similar between the two models, our results also showed some parameters which had different and even opposite responses between the *hsla*-knockout and HSL-IN-1-treated fish. We noticed that in the 5-week feeding trial, the *hsla*^{-/-} zebrafish showed retarded growth; however, enzymic inhibition of Hsl did not significantly reduce growth. Considering the inhibiting efficiency of biochemical inhibitor is normally lower than the gene-knockout method⁽⁷⁰⁾, the 5-week inhibitor feeding was probably not longer enough to show significant difference in growth. In addition, the *hsla*-knockout and HSL-IN-1-treated fish both exhibited lipid accumulation in liver. The expressions of lipogenesis-related genes, including *sreb1c*, *acc*, *fasn* and *dgat1a*, were significantly increased in the *hsla*-knockout fish compared with WT. This could be a compensatory response induced by the *hsla*-knockout-caused reduction of endogenous fatty acids. However, the expressions of these genes showed the opposite trend in the Hsl-inhibitor-treated fish. In addition, the *hsla*-knockout fish showed enhanced glycogen utilisation, indicating the elevated energy production from carbohydrate rather than lipids, but the HSL-IN-1-treated fish showed higher glycogen accumulation in liver. These inconsistent results could be caused by the differences between complete inhibition (gene knockout) and partial inhibition (biochemical inhibition) of Hsl function^(71–73) or caused the possible side effects of HSL-IN-1 in inhibiting lipogenesis genes and elevating glycogen accumulation. Although these are still waiting for further evaluation, the phenotype differences between genetic and biochemical inhibition for the same enzyme are commonly reported. For example, the *atgl*-knocked fish showed significantly retarded growth compared with WT, whereas the *Atgl*-inhibitor-treated fish exhibited significantly increased weight gain compared with control group^(45,46). In addition, the lipid content of muscle in the *cpt1b*-knockout fish was significantly higher than WT⁽³⁰⁾; however, there was no significant difference in the lipid content of muscle between the control group and *Cpt1*-inhibitor-treated fish⁽⁷⁴⁾. All these indicate the importance to use different animals or cell models in identifying the function of a given gene or protein.

Conclusion

The present results demonstrated that the Hsl dysfunction in zebrafish caused retarded growth and reduced oxygen consumption rate, accompanied with the higher mRNA expressions of the genes related to inflammation and apoptosis in liver and muscle. Moreover, the Hsl dysfunction also induced TAG accumulation in multiple tissues, including liver, muscle, and viscera, and reshaped lipid profile with higher proportions of TAG and DG in total lipids. Furthermore, the Hsl dysfunction decreased the glycogen and protein content in tissues, accompanied with the enhanced breakdown of glucose and protein, and reduced activation of mTOR pathway. Our results illustrate that Hsl is a crucial metabolic enzyme for growth, health and maintenance of nutrient homeostasis in organisms. Therefore, this study could provide valuable insights into the functions of Hsl on nutrition regulation and provide a potential regulatory target to improve animal health.

Acknowledgements

All authors contributed experimental assistance and intellectual input to this study.

This work was financed by the National Natural Science Fund of China (31830102).

Z.-Y. D. and M.-L. Z. conceived the original concept. J.-G. W., Z.-Y. D. and M.-L. Z. designed the experimental strategies and sampling plans. J.-G. W. and S.-H. Z. performed the feeding experiments. J.-G. W., S.-H. Z., Y.-C. Q. and Y.-C. L. contributed to the collection of samples. J.-G. W. performed the molecular and biochemistry detections. Z.-Y. D., M.-L. Z., Y. L. and F.Q. provided essential materials and technical supports. Z.-Y. D., J.-G. W. and Y.-F. Q. drafted and revised the manuscript. All authors read and approved the final manuscript.

All authors declare no conflicts of interests.

Supplementary material

For supplementary material/s referred to in this article, please visit <https://doi.org/10.1017/S0007114522003622>

References

- Peirce V, Carobbio S & Vidal-Puig A (2014) The different shades of fat. *Nature* **510**, 76–83.
- Cerk IK, Wechselberger L & Oberer M (2017) Adipose triglyceride lipase regulation: an overview. *Curr Protein Pept Sci* **19**, 221–233.
- Amer P & Langin D (2014) Lipolysis in lipid turnover, cancer cachexia, and obesity-induced insulin resistance. *Trends Endocrinol Metab* **25**, 255–262.
- Zechner R, Zimmermann R, Eichmann TO, *et al.* (2012) FAT SIGNALS—lipases and lipolysis in lipid metabolism and signaling. *Cell Metab* **15**, 279–291.
- Montagner A, Polizzi A, Fouché E, *et al.* (2016) Liver PPAR α is crucial for whole-body fatty acid homeostasis and is protective against NAFLD. *Gut* **65**, 1202–1214.
- Schweiger M, Schreiber R, Haemmerle G, *et al.* (2006) Adipose triglyceride lipase and hormone-sensitive lipase are the major enzymes in adipose tissue triacylglycerol catabolism. *J Biol Chem* **281**, 40236–40241.
- Lafontan M & Langin D (2009) Lipolysis and lipid mobilization in human adipose tissue. *Prog Lipid Res* **48**, 275–297.
- Reczens E, Mouisel E & Langin D (2021) Hormone-sensitive lipase: sixty years later. *Prog Lipid Res* **82**, 101084.
- Haemmerle G, Moustafa T, Woelkart G, *et al.* (2011) ATGL-mediated fat catabolism regulates cardiac mitochondrial function via PPAR- α and PGC-1. *Nat Med* **17**, 1076–1085.
- Granneman JG, Moore HP, Krishnamoorthy R, *et al.* (2009) Perilipin controls lipolysis by regulating the interactions of AB-hydrolase containing 5 (Abhd5) and adipose triglyceride lipase (Atgl). *J Biol Chem* **284**, 34538–34544.
- Gaidhu MP, Anthony NM, Patel P, *et al.* (2010) Dysregulation of lipolysis and lipid metabolism in visceral and subcutaneous adipocytes by high-fat diet: role of ATGL, HSL, and AMPK. *Am J Physiol Cell Physiol* **298**, C961–971.
- Harada K, Shen WJ, Patel S, *et al.* (2003) Resistance to high-fat diet-induced obesity and altered expression of adipose-specific genes in HSL-deficient mice. *Am J Physiol Endocrinol Metab* **285**, E1182–1195.
- Lampidonis AD, Rogdakis E, Voutsinas GE, *et al.* (2011) The resurgence of Hormone-Sensitive Lipase (HSL) in mammalian lipolysis. *Gene* **477**, 1–11.
- Scalvini L, Piomelli D & Mor M (2016) Monoglyceride lipase: structure and inhibitors. *Chem Phys Lipids* **197**, 13–24.
- Garton AJ, Campbell DG, Cohen P, *et al.* (1988) Primary structure of the site on bovine hormone-sensitive lipase phosphorylated by cyclic AMP-dependent protein kinase. *FEBS Lett* **229**, 68–72.
- Tsiloulis T & Watt MJ (2015) Exercise and the regulation of adipose tissue metabolism. *Prog Mol Biol Transl Sci* **135**, 175–201.
- Kim BY, Yoo W, Huong Luu Le LT, *et al.* (2019) Characterization and mutation analysis of a cold-active bacterial hormone-sensitive lipase from *Salinisphaera* sp. P7–4. *Arch Biochem Biophys* **663**, 132–142.
- Krintel C, Osmark P, Larsen MR, *et al.* (2008) Ser649 and Ser650 are the major determinants of protein kinase A-mediated activation of human hormone-sensitive lipase against lipid substrates. *PLoS One* **3**, e3756.
- Albert JS, Yerges-Armstrong LM, Horenstein RB, *et al.* (2014) Null mutation in hormone-sensitive lipase gene and risk of type 2 diabetes. *N Engl J Med* **370**, 2307–2315.
- Mulder H, Sorhede-Winzell M, Contreras JA, *et al.* (2003) Hormone-sensitive lipase null mice exhibit signs of impaired insulin sensitivity whereas insulin secretion is intact. *J Biol Chem* **278**, 36380–36388.
- Roduit R, Masiello P, Wang SP, *et al.* (2001) A role for hormone-sensitive lipase in glucose-stimulated insulin secretion: a study in hormone-sensitive lipase-deficient mice. *Diabetes* **50**, 1970–1975.
- Xia B, Cai GH, Yang H, *et al.* (2017) Adipose tissue deficiency of hormone-sensitive lipase causes fatty liver in mice. *PLoS Genet* **13**, e1007110.
- Wang SP, Laurin N, Himms-Hagen J, *et al.* (2001) The adipose tissue phenotype of hormone-sensitive lipase deficiency in mice. *Obes Res* **9**, 119–128.
- Haemmerle G, Zimmermann R, Hayn M, *et al.* (2002) Hormone-sensitive lipase deficiency in mice causes diglyceride accumulation in adipose tissue, muscle, and testis. *J Biol Chem* **277**, 4806–4815.
- Marshall S (2006) Role of insulin, adipocyte hormones, and nutrient-sensing pathways in regulating fuel metabolism and energy homeostasis: a nutritional perspective of diabetes, obesity, and cancer. *Sci STKE* **2006**, re7.
- Walker C, Sugden M, Gibbons G, *et al.* (2007) Peroxisome proliferator-activated receptor α deficiency modifies glucose handling by isolated mouse adipocytes. *J Endocrinol* **193**, 39–43.
- Burri L, Thoresen GH & Berge RK (2010) The role of PPAR activation in liver and muscle. *PPAR Res* **2010**, 542359.
- Cha DR, Han JY, Su DM, *et al.* (2007) Peroxisome proliferator-activated receptor- α deficiency protects aged mice from insulin resistance induced by high-fat diet. *Am J Nephrol* **27**, 479–482.
- Desai A, Singh R, Sapkale P, *et al.* (2010) Effects of feed supplementation with L-carnitine on growth and body composition of Asian catfish, *Clarias batrachus* fry. *J Appl Anim Res* **38**, 153–157.
- Li L-Y, Li J-M, Ning L-J, *et al.* (2020) Mitochondrial fatty acid β -oxidation inhibition promotes glucose utilization and protein deposition through energy homeostasis remodeling in fish. *J Nutr* **150**, 2322–2335.
- Morigny P, Houssier M, Mouisel E, *et al.* (2016) Adipocyte lipolysis and insulin resistance. *Biochimie* **125**, 259–266.
- Den Broeder MJ, Kopylova VA, Kamminga LM, *et al.* (2015) Zebrafish as a model to study the role of peroxisome proliferator-activated receptors in adipogenesis and obesity. *PPAR Res* **2015**, 358029.
- Lu DL, Ma Q, Wang J, *et al.* (2019) Fasting enhances cold resistance in fish through stimulating lipid catabolism and autophagy. *J Physiol* **597**, 1585–1603.

34. Naser FJ, Jackstadt MM, Fowle-Grider R, *et al.* (2021) Isotope tracing in adult zebrafish reveals alanine cycling between melanoma and liver. *Cell Metab* **33**, 1493–1504.e1495.
35. Quinlivan VH & Farber SA (2017) Lipid uptake, metabolism, and transport in the larval zebrafish. *Front Endocrinol* **8**, 319.
36. Li L-Y, Lu D-L, Jiang Z-Y, *et al.* (2020) Dietary L-carnitine improves glycogen and protein accumulation in Nile tilapia via increasing lipid-sourced energy supply: an isotope-based metabolic tracking. *Aquacult Rep* **17**, 100302.
37. Yan J, Liao K, Wang T, *et al.* (2015) Dietary lipid levels influence lipid deposition in the liver of large yellow croaker (*Larimichthys crocea*) by regulating lipoprotein receptors, fatty acid uptake and triacylglycerol synthesis and catabolism at the transcriptional level. *PLoS One* **10**, e0129937.
38. Liu D, Mai K & Ai Q (2015) Tumor necrosis factor α is a potent regulator in fish adipose tissue. *Aquacult* **436**, 65–71.
39. Chen QL, Luo Z, Song YF, *et al.* (2014) Hormone-sensitive lipase in yellow catfish *Pelteobagrus fulvidraco*: molecular characterization, mRNA tissue expression and transcriptional regulation by leptin *in vivo* and *in vitro*. *Gen Comp Endocrinol* **206**, 130–138.
40. Sun J, Ji H, Li XX, *et al.* (2016) Lipolytic enzymes involving lipolysis in Teleost: synteny, structure, tissue distribution, and expression in grass carp (*Ctenopharyngodon idella*). *Comp Biochem Physiol B: Biochem Mol Biol* **198**, 110–118.
41. Cruz-Garcia L, Sanchez-Gurmaches J, Bouraoui L, *et al.* (2011) Changes in adipocyte cell size, gene expression of lipid metabolism markers, and lipolytic responses induced by dietary fish oil replacement in gilthead sea bream (*Sparus aurata* L.). *Comp Biochem Physiol A Mol Integr Physiol* **158**, 391–399.
42. Hu Y, Huang Y, Tang T, *et al.* (2020) Effect of partial black soldier fly (*Hermetia illucens* L.) larvae meal replacement of fish meal in practical diets on the growth, digestive enzyme and related gene expression for rice field eel (*Monopterus albus*). *Aquacult Rep* **17**, 100345.
43. Jin M, Pan T, Tocher DR, *et al.* (2019) Dietary choline supplementation attenuated high-fat diet-induced inflammation through regulation of lipid metabolism and suppression of NF κ B activation in juvenile black seabream (*Acanthopagrus schlegelii*). *J Nutr Sci* **8**, e38.
44. Jin M, Lu Y, Yuan Y, *et al.* (2017) Regulation of growth, antioxidant capacity, fatty acid profiles, hematological characteristics and expression of lipid related genes by different dietary n-3 highly unsaturated fatty acids in juvenile black seabream (*Acanthopagrus schlegelii*). *Aquacult* **471**, 55–65.
45. Han SL, Qian YC, Limbu SM, *et al.* (2021) Lipolysis and lipophagy play individual and interactive roles in regulating triacylglycerol and cholesterol homeostasis and mitochondrial form in zebrafish. *Biochim Biophys Acta, Mol Cell Biol Lipids* **1866**, 158988.
46. Han SL, Liu Y, Limbu SM, *et al.* (2021) The reduction of lipid-sourced energy production caused by ATGL inhibition cannot be compensated by activation of HSL, autophagy, and utilization of other nutrients in fish. *Fish Physiol Biochem* **47**, 173–188.
47. Li LY, Limbu SM, Ma Q, *et al.* (2018) The metabolic regulation of dietary L-carnitine in aquaculture nutrition: present status and future research strategies. *Rev Aquacult* **11**, 1228–1257.
48. Abo Alrob O & Lopuschuk GD (2014) Role of CoA and acetyl-CoA in regulating cardiac fatty acid and glucose oxidation. *Biochem Soc Trans* **42**, 1043–1051.
49. Han S-L, Wang J, Li L-Y, *et al.* (2020) The regulation of rapamycin on nutrient metabolism in Nile tilapia fed with high-energy diet. *Aquacult* **520**, 734975.
50. Karpac J & Jasper HJC (2011) Metabolic homeostasis: HDACs take center stage. *Cell* **145**, 497–499.
51. Rose S, Frye RE, Slattery J, *et al.* (2014) Oxidative stress induces mitochondrial dysfunction in a subset of autism lymphoblastoid cell lines in a well-matched case control cohort. *PLoS One* **9**, e85436.
52. Horikoshi Y, Yan Y, Terashvili M, *et al.* (2019) Fatty acid-treated induced pluripotent stem cell-derived human cardiomyocytes exhibit adult cardiomyocyte-like energy metabolism phenotypes. *Cells* **8**, 1095.
53. Pajed L, Taschler U, Tilp A, *et al.* (2021) Advanced lipodystrophy reverses fatty liver in mice lacking adipocyte hormone-sensitive lipase. *Commun Biol* **4**, 1–13.
54. Haemmerle G, Lass A, Zimmermann R, *et al.* (2006) Defective lipolysis and altered energy metabolism in mice lacking adipose triglyceride lipase. *Science* **312**, 734–737.
55. Fischer J, Lefevre C, Morava E, *et al.* (2007) The gene encoding adipose triglyceride lipase (PNPLA2) is mutated in neutral lipid storage disease with myopathy. *Nat Genet* **39**, 28–30.
56. Park SY, Kim HJ, Wang S, *et al.* (2005) Hormone-sensitive lipase knockout mice have increased hepatic insulin sensitivity and are protected from short-term diet-induced insulin resistance in skeletal muscle and heart. *Am J Physiol Endocrinol Metab* **289**, E30–E39.
57. Voshol PJ, Haemmerle G, Ouwens DM, *et al.* (2003) Increased hepatic insulin sensitivity together with decreased hepatic triglyceride stores in hormone-sensitive lipase-deficient mice. *Endocrinology* **144**, 3456–3462.
58. Girousse A, Tavernier G, Valle C, *et al.* (2013) Partial inhibition of adipose tissue lipolysis improves glucose metabolism and insulin sensitivity without alteration of fat mass. *PLoS Biol* **11**, e1001485.
59. Morigny P, Houssier M, Mairal A, *et al.* (2019) Interaction between hormone-sensitive lipase and ChREBP in fat cells controls insulin sensitivity. *Nat Metab* **1**, 133–146.
60. Inoki K, Corradetti MN & Guan KL (2005) Dysregulation of the TSC-mTOR pathway in human disease. *Nat Genet* **37**, 19–24.
61. Wang X & Proud CG (2006) The mTOR pathway in the control of protein synthesis. *Physiology* **21**, 362–369.
62. Targher G, Bertolini L, Scala L, *et al.* (2005) Non-alcoholic hepatic steatosis and its relation to increased plasma biomarkers of inflammation and endothelial dysfunction in non-diabetic men. Role of visceral adipose tissue. *Diabetic Med* **22**, 1354–1358.
63. Hijona E, Hijona L, Arenas JI, *et al.* (2010) Inflammatory mediators of hepatic steatosis. *Mediat Inflamm* **2010**, 837419.
64. Cheng J, Yang Z, Ge XY, *et al.* (2022) Autonomous sensing of the insulin peptide by an olfactory G protein-coupled receptor modulates glucose metabolism. *Cell Metab* **34**, 240–255.e210.
65. Cinti S, Mitchell G, Barbatelli G, *et al.* (2005) Adipocyte death defines macrophage localization and function in adipose tissue of obese mice and humans. *J Lipid Res* **46**, 2347–2355.
66. Peng Y, French BA, Tillman B, *et al.* (2014) The inflammasome in alcoholic hepatitis: its relationship with Mallory–Denk body formation. *Exp Mol Pathol* **97**, 305–313.
67. Szabo G & Petrasek J (2015) Inflammasome activation and function in liver disease. *Nat Rev Gastroenterol Hepatol* **12**, 387–400.
68. Mandrekar P & Szabo G (2009) Signalling pathways in alcohol-induced liver inflammation. *J Hepatol* **50**, 1258–1266.
69. Kayagaki N, Wong MT, Stowe IB, *et al.* (2013) Noncanonical inflammasome activation by intracellular LPS independent of TLR4. *Science* **341**, 1246–1249.
70. Rossi JL, Velentza AV, Steinhorn DM, *et al.* (2007). MLCK210 gene knockout or kinase inhibition preserves lung function



- following endotoxin-induced lung injury in mice. *Am J Physiol Lung Cell Mol Physiol* **292**, L1327–L1334.
71. Iborra FJ, Jackson, DA & Cook PR (2001) Coupled transcription and translation within nuclei of mammalian cells. *Science* **293**, 1139–1142.
 72. Galli-Taliadoros LA, Sedgwick JD, Wood SA, *et al.* (1995) Gene knock-out technology: a methodological overview for the interested novice. *J Immunol Methods* **181**, 1–15.
 73. Ogiyama T, Yamaguchi M, Kurikawa N, *et al.* (2017) Identification of a novel hormone sensitive lipase inhibitor with a reduced potential of reactive metabolites formation. *Bioorgan Med Chem* **25**, 2234–2243.
 74. Li LY, Wang Y, Limbu SM, Li JM, *et al.* (2021) Reduced fatty acid β -oxidation improves glucose catabolism and liver health in Nile tilapia (*Oreochromis niloticus*) juveniles fed a high-starch diet. *Aquaculture* **535**, 736392.

